

LUMINOUS BLUE VARIABLES AT QUIESCENCE: THE ZONE OF AVOIDANCE IN THE HERTZSPRUNG-RUSSELL DIAGRAM

RICHARD B. STOTHERS AND CHAO-WEN CHIN

Institute for Space Studies, NASA/Goddard Space Flight Center, 2880 Broadway, New York, NY 10025

Received 1993 December 10; accepted 1994 February 14

ABSTRACT

Two phases of dynamical instability are theoretically predicted to exist during the evolution of supergiants of normal metallicity that are initially more massive than $\sim 60 M_{\odot}$. One phase occurs briefly in the yellow or red region of the Hertzsprung-Russell diagram for stars in the early stages of core helium burning, and the other phase occurs for a longer time in the blue or blue-white region for stars exhausting their core helium. Probably only the second phase exists in the case of supergiants with initial masses between $\sim 60 M_{\odot}$ and $\sim 30 M_{\odot}$ or with low metallicities. The cause of instability is the partial ionization of hydrogen and helium in a quasi-isolated outer region of the stellar envelope, above the layer where the iron opacity attains a large local maximum. Predicted luminosities, effective temperatures, ejected nebular masses, remnant masses, eruption recurrence times, and lifetimes, though very approximate, are generally consistent with available observational data for the important class of unstable supergiants known as luminous blue variables.

Subject headings: stars: evolution — stars: oscillations — stars: variables: other

1. INTRODUCTION

The luminous blue variables (also known as Hubble-Sandage or S Dor variables) present a number of long-standing interpretational puzzles. The biggest puzzle of all is: What is the source of their massive outbursts? Why are their quiescent states characterized, in nearly all cases, by moderately high effective temperatures, $(1-3) \times 10^4$ K, and very high luminosities, greater than $2 \times 10^5 L_{\odot}$ (Humphreys 1989; Wolf 1989)? And why are these locations on the Hertzsprung-Russell (H-R) diagram close to, yet not identical with, the boundary of an apparently forbidden zone, devoid of cool, luminous stars of any kind (Humphreys & Davidson 1979; Blaha & Humphreys 1989)?

Very recently, a classic example of dynamical instability has been discovered to lie within the subphotospheric layers of models of very massive, evolved supergiants (Stothers & Chin 1993, hereafter SC93). Showing promise of accounting for the outbursts of the luminous blue variables, this dynamical instability arises from a complex interplay between the effects of prior stellar wind mass loss, high radiation pressure, partial ionization of hydrogen and helium, and large iron opacities, which cause the outer envelope layers cooler than $\sim 5 \times 10^5$ K effectively to float on a powerful radiation field, virtually isolated from the rest of the star. When these layers become dynamically unstable, they detach from the underlying star in a series of violent relaxation oscillations. Although the main aspects of this interpretation of the luminous blue variables had been inferred earlier (Stothers & Chin 1983), there had always been an unknown missing ingredient—the large iron opacities, which were only discovered a few years afterwards (Iglesias, Rogers, & Wilson 1987).

In this *Letter* we map in detail the occurrence of the classical dynamical instability across the H-R diagram. Sufficient resolution is obtained to suggest plausible answers to all three questions posed above.

2. PHYSICAL ASSUMPTIONS

The same physical input parameters are used here as in SC93. Briefly, we employ the new Livermore opacities (Iglesias,

Rogers, & Wilson 1992), the Ledoux criterion for convection and semiconvection, no convective overshooting, $\alpha_p = 1.4$ as the convective mixing-length parameter, and $X_e = 0.700$ and $Z_e = 0.03$ as the initial hydrogen and metals abundances by mass. A minor computational improvement has been introduced into our solution of the mixing-length equations for very low density conditions and yields some small differences from our earlier published stellar models. We have also studied the consequences of selecting Z_e between 0.015 and 0.03, and α_p between 1.4 and 1.8, but have obtained no important change of model results.

In the present study, initial stellar masses are taken to be 30, 45, 60, 90, and $120 M_{\odot}$. Stellar wind mass loss is included in our models at a rate given, as before, by an analytic formula fitted to the observed rates of mass loss for Galactic stars (Nieuwenhuijzen & de Jager 1990), but multiplied here by a constant factor, w , to allow some uncertainty that was not taken into account in SC93. The formula fit has a standard deviation of about a factor of 2, which is comparable to the estimated (1σ) internal accuracy of the measured mass-loss rates for individual stars (de Jager, Nieuwenhuijzen, & van der Hucht 1988; Lamers & Leitherer 1993). Since stars of the extreme brightness considered here are very rare, the systematic uncertainty of the adopted formula for the rate could easily be as large as a factor of ~ 4 . Wolf-Rayet mass-loss rates are not employed, because the envelopes of our models remain sufficiently cool and sufficiently hydrogen-rich that such rates may not be applicable (Conti, Leep, & Perry 1983; Hamann, Koesterke, & Wessolowski 1993). We adopt $w = 0, 0.25, 0.50, 1, 2$, and 4.

No correction has been applied to the model effective temperatures to allow for the presence of a pseudophotosphere created by the stellar wind (de Loore, Hellings, & Lamers 1982; Schaller et al. 1992). The amount of apparent temperature reduction is extremely uncertain (Hamann et al. 1993), and the empirical effective temperatures of luminous blue variables are already inferred with some partial allowance for the stellar wind.

All of the present stellar models were tested for dynamical instability by computing the pressure-weighted volumetric

average of the first generalized adiabatic exponent, $\langle \Gamma_1 \rangle$, in the outer part of the envelope, and by seeing whether this quantity is less than $4/3$. In SC93 we verified by linear adiabatic pulsation theory that the condition $\langle \Gamma_1 \rangle = 4/3$ does in fact indicate the onset of dynamical instability.

3. DYNAMICAL INSTABILITY

3.1. First Phase

Evolutionary tracks for the stars with the highest initial masses are plotted on the H-R diagram in Figure 1; to avoid confusion, only four tracks appear for each initial mass. These tracks run from the zero-age main sequence into the early stages of core helium ignition. They agree very closely with the tracks computed by Kiriakidis, Fricke, & Glatzel (1993) under similar assumptions, but not with those of Schaller et al. (1992) and Bressan et al. (1993), who assumed a moderate amount of convective core overshooting and, for low surface hydrogen abundances, Wolf-Rayet mass-loss rates. Although these last two sets of evolutionary tracks disagree in many respects between each other, they consistently avoid the yellow and red regions of the H-R diagram for initial masses greater than $\sim 60 M_\odot$. For those two sets of tracks, dynamical instability of the outer envelope could occur, if at all, only in the blue region. We emphasize that in the case of such high stellar masses relatively small changes in input parameters, and even in computational accuracy, can sometimes lead to exaggerated differences in the resulting evolutionary tracks.

A dot plotted along our tracks in Figure 1 indicates when dynamical instability is first encountered; cooler sections of these tracks contain only unstable models. The critical models possess $X_{\text{surf}} = 0.2$ – 0.4 , near-equilibrium abundances of CNO-processed metals at the surface, and stellar masses reduced by about a half. Dynamical instability, when it develops, usually occurs several thousand years after the end of central hydrogen burning, while the star is rapidly crossing the H-R diagram. A curious exception occurs for the $120 M_\odot$ sequences with $w = 0.25$ and 0.50 , which become relatively cool and dynami-

cally unstable during the main-sequence phase itself. All of the unstable models show effective temperatures lower than $12,000$ K.

Stellar wind mass loss is needed to produce dynamical instability. In terms of the parameter w , the minimum rate required is ~ 0.2 , ~ 0.4 , and ~ 4 for initial stellar masses of 120 , 90 , and $60 M_\odot$, respectively. These are all observationally permitted values. For initial masses below $\sim 60 M_\odot$, the evolutionary sequences running up to core helium ignition remain dynamically stable regardless of the value of w . The smallest luminosity to show instability in the yellow region is $\sim 6 \times 10^5 L_\odot$.

When mass loss starts to become substantial, the star thermally readjusts by shrinking its radius, eventually becoming a blue supergiant. If the mass of the retained envelope is sufficiently large, the envelope's secular readjustment requires several decades, but an envelope of small mass can readjust in just a few years, according to our previously published evolutionary simulations (Stothers & Chin 1983, Figs. 1 and 2). Disequilibrium of the envelope might lead to cyclic outbursts for a while. During this time, the bolometric luminosity L remains nearly constant, because the total available recombination energy of hydrogen and helium in the outer envelope for such a luminous star is small compared to $L \Delta t$, where $\Delta t \sim 1$ – 10^2 yr. If, however, the expelled envelope is sufficiently massive, the ultimate release of its thermal and radiative energy content could substantially increase the observed L of the whole object, as Davidson (1989) has argued for η Car. The dynamical instability may recur, but the number of such recurrences must be very small, as the time required for reexpansion of the envelope after each episode is comparable to the total duration of the core contraction phase, before helium burning secularly stabilizes the whole star.

How well do these predictions hold up in a comparison with observations? We will use here the collected data for the quiescent-state characteristics of eight well-studied luminous blue variables from Table 2 of Humphreys (1989; see also Humphreys et al. 1989). They will be supplemented with data for the four additional variables HR Car (van Genderen et al. 1991; Hutsemékers & Van Drom 1991a), WRA 751 (Hu et al. 1990; Hutsemékers & Van Drom 1991b; van Genderen et al. 1992), R 110 (Stahl et al. 1990), and R 143 (Parker et al. 1993). These 12 stars are plotted on the H-R diagram in Figure 2. Although all of our present models (shown by filled circles) appear to be unacceptably cool, they represent only stars at the onset of dynamical instability, not during their subsequent quiescent periods. There exists some circumstantial evidence that just before their major outbursts a few centuries ago the now-blue variables P Cyg (Lamers & de Groot 1992) and AG Car (Robberto et al. 1993) were actually yellow supergiants. Variable A in M33 also appears to be intrinsically a yellow or red supergiant (Humphreys, Jones, & Gehrz 1987; Humphreys 1989). De Jager & van Genderen (1989) have mentioned several other peculiar yellow supergiants that may belong to this class. Unfortunately, nothing is known about the color of η Car before its great outburst in the last century (O'Connell 1956; van Genderen & Thé 1984). Those luminous blue variables that are brighter than $\sim 6 \times 10^5 L_\odot$ and were once yellow supergiants may correspond to our present models.

Most of the other luminous blue variables, however, are either known or strongly suspected to be blue supergiants before their outbursts, like Variable C in M33 and the five well-studied members of the Large Magellanic Cloud (S Dor, R 71, R 110, R 127, and R 143). Moreover, at least three of the

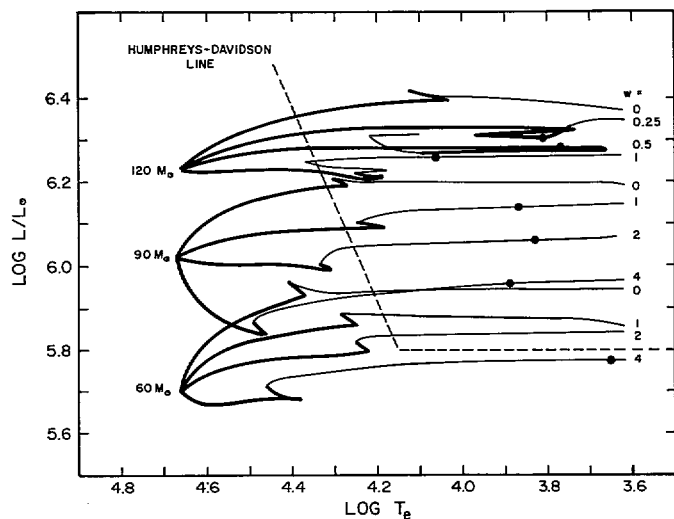


FIG. 1.—H-R diagram showing evolutionary tracks running from the zero-age main sequence to the onset of core helium burning. The slow phase of core hydrogen burning is indicated by the thick lines. Tracks are labeled with the initial stellar mass and with the stellar wind mass-loss parameter w . A dot indicates the bluest stage for which dynamical instability occurs in the outer envelope.

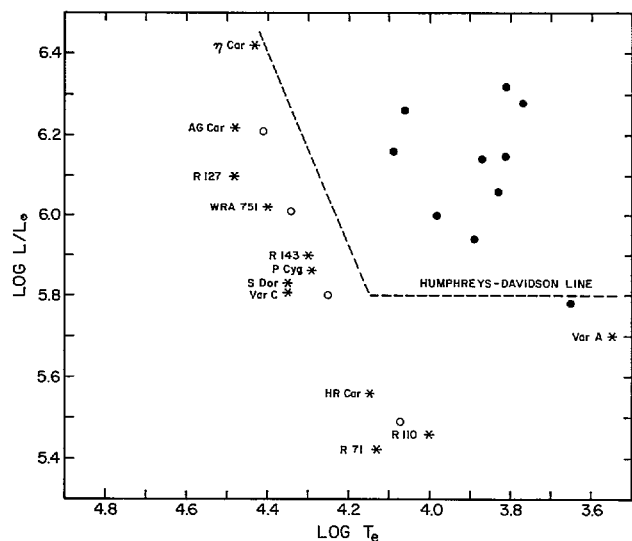


FIG. 2.—H-R diagram showing the location of stellar models at the onset of dynamical instability: first unstable phase, filled circles; second unstable phase, open circles. The published locations of luminous blue variables at quiescence are also shown (asterisks), although these locations have considerable uncertainty.

variables (HR Car, R 71, and R 110) are incontrovertibly too faint with respect to our present models.

It is possible that the faintest luminous blue variables have reached their present positions on the H-R diagram as a consequence of heavy stellar wind mass loss in the red-supergiant region during the early stages of core helium burning (Lamers, de Groot, & Cassatella 1983). Termination of the red phase, however, might have come prematurely. As the wind carried off mass, the outer envelope would have gradually approached the threshold of dynamical instability. We find that this threshold can actually be crossed for initial masses as low as $\sim 60 M_{\odot}$, although the uncertainty of this critical mass is possibly a factor of 2 because the Nieuwenhuijzen & de Jager (1990) rate of stellar wind mass loss may be uncertain by a factor of as much as 10 either way in the red region (Dupree 1986, Fig. 13). The moderately faint Variable A in M33 is a possible example of such a dynamically unstable red supergiant.

The instantaneous mass of the unstable outer envelope in our models ranges from $\sim 10^{-2} M_{\odot}$ for an F-type supergiant to $\sim 1 M_{\odot}$ for an M-type supergiant. Since dynamical instability feeds on itself and only ceases when the underlying envelope layers begin to shrink (SC93), the total amount of mass lost during an eruptive episode may well exceed these crude estimates. Nevertheless, it is interesting to find that the old dust nebulae detected around η Car and AG Car, which might have been yellow or red supergiants just prior to their associated outbursts, contain total masses of $\sim 2 M_{\odot}$ (Lamers 1989). These observed masses have an uncertainty of a factor of 10, but probably not more than this. The stars' estimated recurrence times of $\sim 10^3$ yr (Lamers 1989) are also consistent with our predictions.

3.2. Second Phase

Blocked dynamically from dwelling in the yellow and red regions, a very massive star has to settle down, rather quickly, into steady core helium burning as a blue supergiant. This stable phase can last up to 3×10^5 yr and is accompanied by further stellar wind mass loss. When central helium runs low

($Y_c < 0.1-0.3$), the envelope starts a new phase of reexpansion on an accelerated timescale. This time, however, dynamical instability sets in at a hotter effective temperature, because the star's increased luminosity-to-mass ratio raises the contribution of radiation pressure to the total pressure and thereby reduces the amount of hydrogen and helium partial ionization needed to bring $\langle \Gamma_1 \rangle$ below 4/3. The specific models that we display (as open circles) in Figure 2 have been obtained for the case of remnant envelopes that are somewhat more than minimally massive enough to reexpand. The total stellar mass is only one-third to one-half of the initial mass, and $X_{\text{surf}} \approx 0.2$. Since we find relatively little sensitivity of our results to the detailed structure of the underlying star or to how the star got into this state, we have not depicted any actual evolutionary tracks in the blue region, which are arbitrary at best. On the H-R diagram, the critically unstable models, which are plotted for initial stellar masses of 30, 45, 60, and $90 M_{\odot}$, lie very close to the observed positions of the luminous blue variables at quiescence (Fig. 2). The predicted masses, represented satisfactorily by $\log (M/M_{\odot}) = 0.81 \log (L/L_{\odot}) - 3.42$, also agree very well with the low atmospherically derived masses.

Supergiants so highly evolved are theoretically barred from passing the line of open circles on Figure 2. Repeated attempts of the envelope to expand more fully are thwarted by sudden encounters with dynamical instability that leads to mass ejection. The recurrence time depends on how far the postoutburst star retreats to the blue of the instability line, and so could be as little as ~ 1 yr or as much as $\sim 10^2$ yr. The minimum mass lost in an eruptive episode can be estimated from the instantaneous mass of the dynamically unstable part of the envelope, 10^{-6} to $10^{-4} M_{\odot}$ for blue to blue-white supergiants. The total duration of this unstable stage of evolution cannot exceed the lifetime of core helium burning and later phases, $\sim 3 \times 10^5$ yr, and is probably only 0.1–0.3 as long. In spite of the theoretical uncertainties, our predictions seem to be consistent with what is empirically known about the equilibrium properties and cyclic outbursts of luminous blue variables that show blue precursors (Lamers 1989).

Last, we point out that stars with initial masses less than $\sim 30 M_{\odot}$ probably do not lose enough mass to encounter this dynamical instability. For example, the blue supergiant that became SN 1989A in the Large Magellanic Cloud evolved from a main-sequence star of $\sim 20 M_{\odot}$, and, at the end, possessed an envelope mass of at least $\sim 5 M_{\odot}$ (Arnett et al. 1989). Our models indicate that this star's envelope was much too massive to have ever been dynamically unstable. Indeed, the luminosities of the faintest known luminous blue variables (Fig. 2) imply initial stellar masses of $\sim 30 M_{\odot}$. The only way in which a fainter blue supergiant might possibly become dynamically unstable is through stripping of its envelope in a close binary mass exchange. This could occur for brighter blue supergiants, too.

4. CONCLUSION

Dynamical instability in the outer envelope is predicted to occur at both the beginning and the end of core helium burning in single stars of normal metallicity that are initially more massive than $\sim 60 M_{\odot}$. On the H-R diagram, the instability appears first among the yellow supergiants (for the most luminous stars) or among the red supergiants (for the less luminous stars) and later among the blue or blue-white supergiants. Stars with initial masses between $\sim 60 M_{\odot}$ and $\sim 30 M_{\odot}$, and stars with low metallicities, probably do not undergo the first

of these two phases of instability (see also SC93). Manifestation of the instability is expected to be a massive outburst, like that seen in luminous blue variables.

According to our results, the actual zone of avoidance for very luminous stars on the H-R diagram is much redder than indicated by the Humphreys-Davidson sloped line. As in SC93, we suggest that the Humphreys-Davidson line probably marks the termination of core hydrogen burning, because further evolution to the red would be so rapid as to be rarely observable.

Although the slow phase of core helium burning has to occur somewhere in the blue-supergiant region, our models do not constrain its precise whereabouts. The B[e] supergiants are a possible site. Their known luminosities closely resemble those of the luminous blue variables; effective temperatures are the same or hotter; estimated lifetimes are greater than $(1-2) \times 10^5$ yr; and a defining characteristic is their anomalous infrared excess, which probably arises from a circumstellar dust shell or disk (Zickgraf 1989; Zickgraf, Stahl, & Wolf 1992). It is not known, however, whether their surfaces contain CNO-processed material. Consequently, we predict the following

evolutionary sequence of stellar types among the most massive stars:

$$O \rightarrow Of \rightarrow YSG \text{ (or RSG)} \rightarrow LBV \rightarrow B[e] \\ \text{(or BSG)} \rightarrow LBV \rightarrow WR? \rightarrow SN .$$

Maeder (1983, 1989), Schaller et al. (1992), and Bressan et al. (1993), on the other hand, have proposed the following: $O \rightarrow Of \rightarrow BSG \rightarrow LBV \rightarrow WR \rightarrow SN$. Since their published evolutionary tracks exhibit no red supergiants with initial masses exceeding $\sim 30 M_{\odot}$ and no yellow supergiants more massive than $\sim 60 M_{\odot}$, testable divergences from our proposed sequence exist, even though it is not yet known for certain whether any of their blue-supergiant models actually become dynamically unstable. Further observational and theoretical work is clearly called for.

We thank F. J. Rogers, C. A. Iglesias, and B. G. Wilson for providing us with tables of their revised opacities. Our work was supported by the NASA Astrophysics Research Program.

REFERENCES

- Arnett, W. D., Bahcall, J. N., Kirshner, R. P., & Woosley, S. E. 1989, *ARA&A*, 27, 629
- Blaha, C., & Humphreys, R. M. 1989, *AJ*, 98, 1598
- Bressan, A., Fagotto, F., Bertelli, G., & Chiosi, C. 1993, *A&AS*, 100, 647
- Conti, P. S., Leep, E. M., & Perry, D. N. 1983, *ApJ*, 268, 228
- Davidson, K. 1989, in *Physics of Luminous Blue Variables*, ed. K. Davidson, A. F. J. Moffat, & H. J. G. L. M. Lamers (Dordrecht: Kluwer), 101
- de Jager, C., Nieuwenhuijzen, H., & van der Hucht, K. A. 1988, *A&AS*, 72, 259
- de Jager, C., & van Genderen, A. M. 1989, in *Physics of Luminous Blue Variables*, ed. K. Davidson, A. F. J. Moffat, & H. J. G. L. M. Lamers (Dordrecht: Kluwer), 127
- de Loore, C., Hellings, P., & Lamers, H. J. G. L. M. 1982, in *IAU Symp. 99, Wolf-Rayet Stars: Observations, Physics, Evolution*, ed. C. W. H. de Loore & A. J. Willis (Dordrecht: Reidel), 53
- Dupree, A. K. 1986, *ARA&A*, 24, 377
- Hamann, W.-R., Koesterke, L., & Wessolowski, U. 1993, *A&A*, 274, 397
- Hu, J. Y., de Winter, D., Thé, P. S., & Pérez, M. R. 1990, *A&A*, 227, L17
- Humphreys, R. M. 1989, in *Physics of Luminous Blue Variables*, ed. K. Davidson, A. F. J. Moffat, & H. J. G. L. M. Lamers (Dordrecht: Kluwer), 3
- Humphreys, R. M., & Davidson, K. 1979, *ApJ*, 232, 409
- Humphreys, R. M., Jones, T. J., & Gehr, R. D. 1987, *AJ*, 94, 315
- Humphreys, R. M., Lamers, H. J. G. L. M., Hoekzema, N., & Cassatella, A. 1989, *A&A*, 218, L17
- Hutsemékers, D., & Van Drom, E. 1991a, *A&A*, 248, 141
- . 1991b, *A&A*, 251, 620
- Iglesias, C. A., Rogers, F. J., & Wilson, B. G. 1987, *ApJ*, 322, L45
- . 1992, *ApJ*, 397, 717
- Kiriakidis, M., Fricke, K. J., & Glatzel, W. 1993, *MNRAS*, 264, 50
- Lamers, H. J. G. L. M. 1989, in *Physics of Luminous Blue Variables*, ed. K. Davidson, A. F. J. Moffat, & H. J. G. L. M. Lamers (Dordrecht: Kluwer), 135
- Lamers, H. J. G. L. M., & de Groot, M. J. H. 1992, *A&A*, 257, 153
- Lamers, H. J. G. L. M., de Groot, M., & Cassatella, A. 1983, *A&A*, 123, L8
- Lamers, H. J. G. L. M., & Leitherer, C. 1993, *ApJ*, 412, 771
- Maeder, A. 1983, *A&A*, 120, 113
- . 1989, in *Physics of Luminous Blue Variables*, ed. K. Davidson, A. F. J. Moffat, & H. J. G. L. M. Lamers (Dordrecht: Kluwer), 15
- Nieuwenhuijzen, H., & de Jager, C. 1990, *A&A*, 231, 134
- O'Connell, D. J. K. 1956, *Vistas Astron.*, 2, 1165
- Parker, J. W., Clayton, G. C., Winge, C., & Conti, P. S. 1993, *ApJ*, 409, 770
- Robberto, M., Ferrari, A., Nota, A., & Paresce, F. 1993, *A&A*, 269, 330
- Schaller, G., Schaerer, D., Meynet, G., & Maeder, A. 1992, *A&AS*, 96, 269
- Stahl, O., Wolf, B., Klare, G., Jüttner, A., & Cassatella, A. 1990, *A&A*, 228, 379
- Stothers, R. B., & Chin, C.-w. 1983, *ApJ*, 264, 583
- . 1993, *ApJ*, 408, L85 (SC93)
- Van Genderen, A. M., Robijn, F. H. A., van Esch, B. P. M., & Lamers, H. J. G. L. M. 1991, *A&A*, 246, 407
- Van Genderen, A. M., & Thé, P. S. 1984, *Space Sci. Rev.*, 39, 317
- Van Genderen, A. M., Thé, P. S., de Winter, D., Hollander, A., de Jong, P. J., van den Bosch, F. C., Kolkman, O. M., & Verheijen, M. A. W. 1992, *A&A*, 258, 316
- Wolf, B. 1989, in *Physics of Luminous Blue Variables*, ed. K. Davidson, A. F. J. Moffat, & H. J. G. L. M. Lamers (Dordrecht: Kluwer), 91
- Zickgraf, F.-J. 1989, in *Physics of Luminous Blue Variables*, ed. K. Davidson, A. F. J. Moffat, & H. J. G. L. M. Lamers (Dordrecht: Kluwer), 117
- Zickgraf, F.-J., Stahl, O., & Wolf, B. 1992, *A&A*, 260, 205